

Local ac magnetic response in type-II superconductors

R. Prozorov, A. Shaulov, Y. Wolfus, and Y. Yeshurun
Department of Physics, Bar-Ilan University, 52900 Ramat-Gan, Israel

(Received 3 May 1994; accepted for publication 16 August 1994)

We present an analysis of the *local* ac magnetic response in type-II superconductors as measured by a miniature Hall probe. The results show that the response is a function of the position of the probe even in a homogeneous sample. The local response in an inhomogeneous sample is further influenced by local variations of superconducting properties across the sample. Applications of this analysis in characterizing and mapping of inhomogeneities in a sample are illustrated. © 1994 American Institute of Physics.

High-temperature superconductors (HTS) in the form of thin films have attracted special interest because of their potential applications in microelectronic devices. A wide variety of techniques have been successfully employed in fabricating and characterizing HTS thin films. However, the characterization techniques commonly employed measure average (global) quantities and provide no information about variations of local properties across the film. Superconducting properties, such as the transition temperature T_c and the shielding current density j_s , may vary across a film as a result of variations in stoichiometry or presence of defects. The development of methods for the detection and elimination of such variations is crucial for successful applications of HTS films in practical devices.

Recently, a preliminary system for local measurements of superconducting properties in thin films has been demonstrated, using a conventional read/write magnetic head mounted on a mechanical scanner.¹ In this technique the third harmonic component of the local AC response was used to generate surface images of several samples; however, no interpretation of these images has been given. More sophisticated spatial-scanning techniques involve direct magneto-optic imaging² and micro-Hall probes.³⁻⁷ The micro-Hall probe technique is suitable for ac measurements and extremely sensitive. Presently, linearly arrays^{5,6} of micro-Hall probes have become available, and two-dimensional arrays are underway. Such arrays will allow fast electronic scanning to create two-dimensional maps of the local dc or ac response of the films.

The aim of this paper is to give a detailed analysis of the *local* ac response, as measured by a miniature Hall probe located on the sample surface at some distance from its edge. Our analysis shows important differences between the ac response at different locations of the Hall probe. Understanding of these differences is important for correct interpretation of the local ac measurements and for the utilization of these measurements in characterizing and mapping of inhomogeneities across the sample.

Our analysis is based on the following assumptions:

- (a) (a) The dimensions of the Hall probe are much smaller than the sample size. Experimentally, a micro-Hall probe with working area as small as $\sim 2 \times 2 \mu\text{m}$ can be realized.⁷ This is much smaller than the planar dimensions of usual samples ($\geq 1000 \mu\text{m}$).
- (b) (b) Variations of the magnitude of the shielding current j_s due to the alternating field H_{ac} can be neglected.

This condition is usually satisfied in experiments using ac fields smaller than the dc field.

Assume now that a miniature Hall probe is located at a distance r from the nearest edge of the sample located at $r=0$, as shown in Fig. 1. Note that the magnetic induction profiles are not necessarily straight lines;^{8,9} we use straight lines in Fig. 1 only for simplicity. We define "a local penetration field" $H^*(r)$ as the first actual ac field at which oscillations of the z component of the magnetic induction B_z reach the Hall probe. Such a definition of H^* is relevant for any geometry, and it takes into account the lower critical field H_{c1} . The field H^* is directly related to the shielding current j_s ; for a homogeneous infinite slab or cylinder with a zero demagnetization factor $H_{inf}^* = (4\pi/c)j_s r$. For a homogeneous thin film:⁹

$$H_{film}^* = (4\pi/c)t(1+\alpha)j_s \operatorname{arccosh}[W/(W-r)],$$

where W is a coordinate of the center of the sample, t is the thickness, and α accounts for the effect of demagnetization. The parameter α depends on the position of the Hall probe and on the geometry of the sample, and it determines the actual magnitude of the ac field on the edge of a sample: $h_{ac} = (H_{ap} + \alpha H^*) \sin(\omega t) = H_{ac} \sin(\omega t)$, where H_{ap} is the amplitude of the applied ac field.

To illustrate the method of calculation, let us consider the response of the Hall probe for the descending part of h_{ac} (see Fig. 1). Down to the field $H_{ext} = H_{dc} + H_{ac} - 2H^*$ the Hall probe does not feel any change of the external field. After this field is reached, $B_z(h_{ac})$ follows the changes in the external field through a quite complicated relationship,⁹ however it quickly converges to a linear dependence. Assuming a linear relationship between B_z and h_{ac} , one can easily calculate the local ac response as a function of time or, what is more convenient, as a function of the phase $\varphi = \omega t$ during one period. Figure 1 shows schematic profiles of the field at five different stages during a complete cycle. The dependence of B_z on the phase φ during the period between these stages is given in Table I. The dc part of B_z is omitted since it does not affect the ac response.

As an illustration, we show in Fig. 2 graphs of $B_z(\varphi)$ as calculated from Table I for $H^*=0$ and for $H^*=H_{ac}/2$. When H^* is zero the magnetic induction follows the external alternating field. In contrast, when H^* is not zero (e.g., $x = \frac{1}{2}$ in Fig. 2) the signal is cut and there is a pronounced phase shift, which is proportional to the ratio $x = H^*/H_{ac}$. Both features, the saturation of the ac signal and a phase shift, were experi-

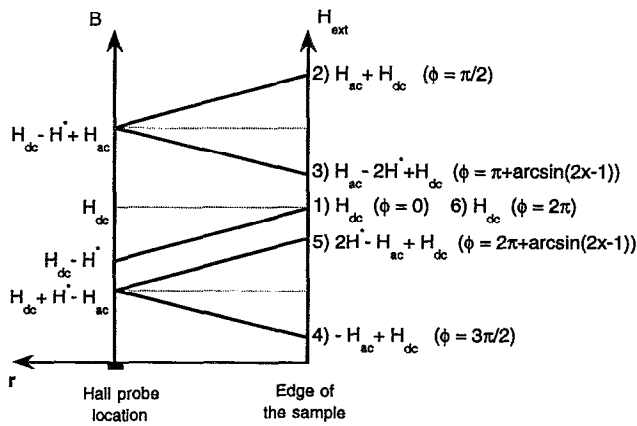


FIG. 1. Schematic description of the magnetic induction during one cycle. Straight lines are only for simplicity of the plot.

mentally observed by Wang and Sayer,¹⁰ although the geometry of their experiment was slightly different. Once the waveform of B_z is known, the real and imaginary parts of the local harmonic susceptibilities, χ'_n and χ''_n , respectively, can be calculated:

$$\begin{cases} \chi'_n \\ \chi''_n \end{cases} = \frac{1}{H_{ac}} \int_0^{2\pi} \begin{cases} \sin(n\varphi) \\ \cos(n\varphi) \end{cases} d\varphi.$$

The results for the first, third, and fifth harmonics are summarized in Table II. In this table $A_n = \sqrt{(\chi'_n)^2 + (\chi''_n)^2}$ is the magnitude of the n th harmonic susceptibility, and $\rho = \sqrt{x(1-x)}$. Even harmonics do not exist in this model due to the symmetrical functional form of $B_z(\varphi)$.

For the experimental verification of these results we measured the ac response of an YBCO thin film (thickness 300 nm) using a 50×50 - μm^2 micro-Hall probe attached to the surface of the film and located at a distance approximately 500 μm from the edge of the sample. The measurements were performed at a fixed temperature ($T=88$ K), dc magnetic field ($H_{dc}=200$ G) and frequency of the ac field ($f=177$ Hz). Figure 3 shows the third and the fifth harmonics (both normalized by H_{ap}) as a function of H_{ap} . Symbols are experimental points and the solid lines are fits calculated using the expressions given in Table II. A good agreement of

TABLE I. Magnetic induction $B_z(\varphi)$ at the Hall-probe location during one cycle of the ac field. The parameter x denotes the ratio H^*/H_{ac} .

Stage No. (see Fig. 1)	φ	$B_z(\varphi)$
1 to 2	$0 \rightarrow \frac{\pi}{2}$	$H_{ac} \sin(\varphi) - H^*$
2 to 3	$\frac{\pi}{2} \rightarrow \pi + \arcsin(2x-1)$	$H_{ac} - H^*$
3 to 4	$\pi + \arcsin(2x-1) \rightarrow \frac{3\pi}{2}$	$H_{ac} \sin(\varphi) + H^*$
4 to 5	$\frac{3\pi}{2} \rightarrow 2\pi + \arcsin(2x-1)$	$H^* - H_{ac}$
5 to 6	$2\pi + \arcsin(2x-1) \rightarrow 2\pi$	$H_{ac} \sin(\varphi) - H^*$

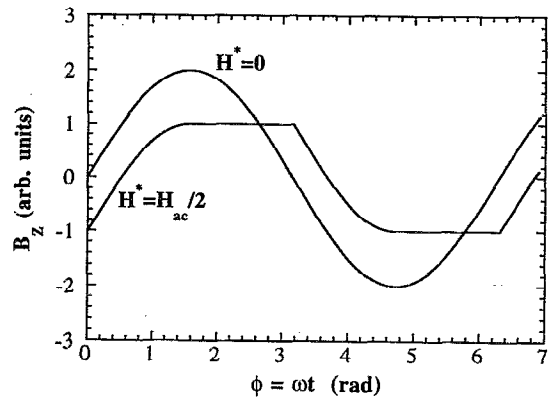


FIG. 2. Curves of $B_z(\varphi)$ as calculated from Table I; for $H^*=0$ and $H^*=H_{ac}/2$.

the experiment with the model is evident. Note that the onset of these local responses is obtained at $H_{ac} \cong 0.3$ G, while the onset of the global response is always obtained at $H_{ac} \rightarrow 0$.

As was pointed out in the introduction, local magnetic ac measurements provide a tool for detecting inhomogeneous regions in the sample. This is illustrated in the following example. Consider a sample with zero demag factor. Its edge is located at $r=0$ and the sample itself occupies the positive part of the r axis. We denote by $r=1$ the maximum propagation distance of the ac field. Suppose that due to some reasons, such as variation of the oxygen content or defects in the microstructure, the shielding current density varies with the coordinate as $j_s(r)$. The penetration field then is given by

TABLE II. Local harmonic susceptibilities χ_n ($n=1,3,5$) normalized by H_{ac} . Here $x=H^*/H_{ac}$ and $\rho = \sqrt{x(1-x)}$.

χ'_1	$\frac{\pi}{2} - 2\rho(2x-1) - \arcsin(2x-1)$
χ''_1	$-4\rho^2$
A_1	$\sqrt{\frac{\pi^2}{4} + 2(2x-1)\rho[2 \arcsin(2x-1) - \pi] + 4\rho^2}$ $+ \arcsin(2x-1)[\arcsin(2x-1) - \pi]$
χ'_3	$\frac{16}{3} \rho^3(2x-1)$
χ''_3	$\frac{4}{3} \rho^2(1-8\rho^2)$
A_3	$\frac{4}{3} \rho^2$
	The maximum $A_3 = \frac{1}{3}$ is reached at $x = \rho = \frac{1}{2}$.
χ'_5	$\frac{16}{15} \rho^3(2x-1)(5-32\rho^2)$
χ''_5	$\frac{4}{15} \rho^2(8\rho^2(9-32\rho^2)-3)$
A_5	$\frac{4}{15} \rho^2 \sqrt{9-32\rho^2}$
	A_5 has two maxima: $A_5 = \frac{\sqrt{3}}{20}$ at $x = \frac{1}{4}$ and $\frac{3}{4}$ and a minimum $A_5 = \frac{1}{15}$ at $x = \frac{1}{2}$.

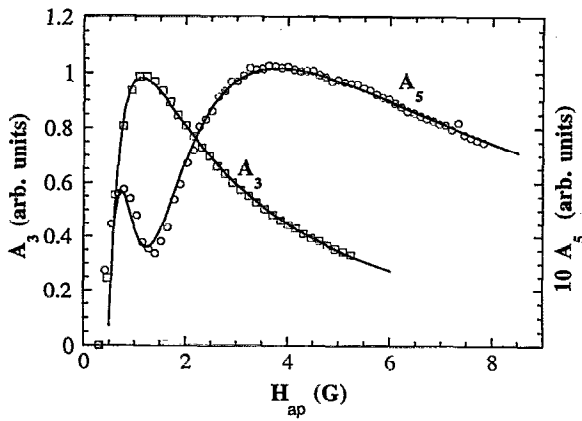


FIG. 3. Third and fifth harmonic signals measured in YBCO thin film as function of H_{ap} at $T=88$ K and $H_{dc}=200$ G. Symbols are experimental data and solid lines are fits.

$$H^*(r) = \frac{4\pi}{c} \int_0^r j_s(\xi) d(\xi).$$

Thus, the shielding current density is simply $j_s(r) = (c/4\pi)[dH^*(r)/dr]$. Therefore, all that we need in order to construct $j_s(r)$ is to measure $H^*(r)$. To obtain $H^*(r)$ at fixed temperature and dc field, one can measure, for instance, $A_3(H_{ac})$ and detect its peak position H_{ac}^{peak} . In general $H_{ac}^{peak} = (1 - \alpha + \sqrt{1 - \alpha})H^*$, thus measurements of H_{ac}^{peak} yield $H^*(r)$. By locating a single Hall probe at different distances r from the edge, or by using a Hall-probes array one can map $H^*(r)$ and hence reconstruct $j_s(r)$. Instead of measuring the peak position of the third harmonic, the same information can be extracted from the magnitude $A_3(r)$ provided H_{ac} is high enough to penetrate the center of the sample. As a specific example, consider three model samples: Sample A is homogeneous, i.e., $j_s = \text{const}$ across the sample; sample B is inhomogeneous such that the shielding current increases from the edge to the center as $j_s(r) = 1/(2-r)$; and sample C has a large defect so that for fractional distance from the edge $r=0.4-0.8$, the shielding current j_s is zero and j_s is 1 in the rest of the material. Figure

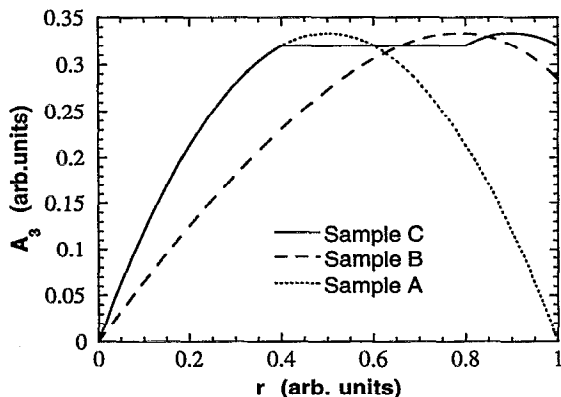


FIG. 4. Spatial variations of the magnitude of third harmonic signals for samples A, B, and C.

4 shows the profiles of the third harmonic amplitude $A_3(r)$ corresponding to samples A, B, and C. Note that for the homogeneous sample A, $A_3(r)$ is *not* constant but rather parabolic. Similarly, in the defect region of sample C, where $j_s=0$, $A_3(r)$ is not zero but rather a finite constant. The relationship between $A_3(r)$ and $j_s(r)$ given in Table II can be reversed to allow mapping of $j_s(r)$ from measurements of $A_3(r)$.

Besides local variations of j_s , one may also measure distribution of other parameters such as the irreversibility temperature T_{irr} .¹¹ Measurements of the onset temperature of the third harmonic signal has been established as a reliable method for determining T_{irr} .¹² Our analysis shows that in a homogeneous sample, while the peak position, height, and width of the third harmonic signal vary as a function of the position r , the *onset* of this signal (on cooling from above T_c) is the same for all positions of the Hall probe. Thus, variations in the onset temperature of the third harmonic signal indicate inhomogeneous distribution of T_{irr} across the sample.

In summary, we have analyzed the local ac response as measured by a miniature Hall probe attached to the surface of the sample. We found that the local response is a function of the position of the probe even in a homogeneous sample. In inhomogeneous samples, the local ac response is further influenced by local variations of superconducting properties across the sample. Our analysis is important for correct interpretation of the local ac measurements and for the utilization of these measurements in characterizing and mapping of inhomogeneities across the sample. We note that for a detailed interpretation of the experimental data one should take into account such factors as surface barrier, finite area of the Hall probe, and finite distance of the Hall probe from the surface of the sample. A full analysis taking into account these factors will be given elsewhere.

We acknowledge valuable discussions with E. Zeldov and Y. Abulafia. This work has been supported by the DG XII, Commission of the European Communities, and the Israeli Ministry of Science and Art.

- ¹R. N. Bhargava, S. P. Herko, and A. Shaulov, *AIP Conference Proceedings*, No. 219 (Fourth Annual Conference on Superconductivity and its Applications, Buffalo, NY, 1990) (American Institute of Physics, New York, 1991).
- ²L. A. Dorosinskii, M. V. Indenbom, V. I. Nikitenko, A. A. Polyanskii, R. L. Prozorov, and V. K. Vlasko-Vlasov, *Physica C* **206**, 360 (1993).
- ³M. Konczykowski, F. Holtzberg, and P. Lejay, *Supercond. Sci. Technol.* **4**, S331 (1991).
- ⁴Y. Wolfus, Y. Abulafia, L. Klein, V. A. Larkin, A. Shaulov, Y. Yeshurun, M. Konczykowski, and M. Feigel'man, *Physica C* **224**, 213 (1994).
- ⁵T. L. Tamegai, L. Krusin-Elbaum, P. Santhanam, M. J. Brady, W. T. Masetink, C. Feild, and F. Holtzberg, *Phys. Rev. B* **45**, 2589 (1992).
- ⁶E. Zeldov, A. I. Larkin, M. Konczykowski, B. Khaykovich, D. Majer, V. B. Geshkenbein, and V. M. Vinokur, *Physica C* (in press).
- ⁷E. Zeldov (private communication).
- ⁸E. H. Brandt and M. Indenbom, *Phys. Rev. B* **48**, 12893 (1993).
- ⁹E. Zeldov, J. R. Clem, M. McElfresh, and M. Darwin, *Phys. Rev. B* **49**, 9802 (1994).
- ¹⁰J. Wang and M. Sayer, *Physica C* **212**, 395 (1993).
- ¹¹For review see A. P. Malozemoff, in *Physical Properties of High Temperature Superconductors*, edited by D. Ginsberg (World Scientific, Singapore, 1989), p. 71.
- ¹²A. Shaulov and D. Dorman, *Appl. Phys. Lett.* **53**, 2680 (1988).